Available online at www.sciencedirect.com
ScienceDirect
Journal of Organometallic Chemistry 691 (2006) 5774–5781
Journal of Organometallic Chemistry
www.elsevier.com/locate/jorganchem

Auto-organization modulation of tetrasubstituted tetrathiafulvalenes (TTF) in silica based hybrid materials

Nathalie Bellec [a,1], Frédéric Lerouge [b,2], Olivier Jeannin [a,1], Geneviève Cerveau [b,2], Robert J.P. Corriu [b,2], Dominique Lorcy [a,*]

[a] Sciences Chimiques de Rennes, UMR 6226 CNRS-Université de Rennes 1, Campus de Beaulieu, Bât 10A, 35042 Rennes Cedex, France
[b] Laboratoire de Chimie Moléculaire et Organisation du Solide, UMR 5637, Université Montpellier II, cc 007, Place E. Bataillon, F-34095 Montpellier Cedex 5, France

Received 27 July 2006; received in revised form 12 September 2006; accepted 12 September 2006
Available online 23 September 2006

Abstract

The effect of the interactions generated by the spacer group between the TTF core and the four triethoxysilane groups on the auto-organization of the organic bridging moieties in hybrid materials obtained by sol–gel chemistry has been investigated. The silica-based hybrid solids are highly polycondensed. They present different scales of organization (nanometric and micrometric) that are independent one from each other and are governed by the different parameters which control the kinetics of polycondensation. Their anisotropic organization is function of the interaction forces induced by the spacer, van der Waals, hydrogen bonding or both, during the hydrolytic condensation process.

Keywords: Tetrathiafulvalene; Cyclic voltammetry; Alkoxysilanes; Sol–gel process; Nanostructured materials

1. Introduction

Molecular organic precursors bearing at least two $Si(OR)_3$ groups can be easily transformed into silica-based hybrid materials by hydrolytic sol–gel polycondensation [1–8]. Moreover it has been shown that a auto-organization in these monophasic hybrid materials occurs spontaneously during the hydrolytic polycondensation regardless the nature and the geometry of the organic units (linear, twisted, planar and even tetrahedral) [9–15]. The organic units present an organization at the nanometric scale evidenced by X-ray powder diffraction, and also at the micrometric scale as shown by birefringence experiments in cross-polarized light microscopy [9–15]. At the present time, two types of auto-organization of organic units inside of the materials are known. The first is induced by van der Waals interactions between organic groups, and the second one is totally different since it results from H-bonding networks. It has been recently shown that the organization due to the lipophilic van der Waals type interactions between the organic moieties is kinetically controlled, as well as the textural properties of the materials [9–15]. Considering the second type of organization, the hydrogen bonds network due to the presence of urea groups, favors the structuring of the hybrid solid [16–22].

Recently, we obtained the first self-organized tetrathiafulvalenes (TTF) in a silica based hybrid organic–inorganic materials prepared by sol–gel chemistry (precursor **1**, Scheme 1) [23,24]. The TTFs used for these studies were substituted by two or four trialkoxysilyl functions linked to the TTF core by a spacer group including a carbamate moiety. The resulting hybrid solids were highly

* Corresponding author. Fax: +33 2 23 23 67 38.
E-mail address: Dominique.Lorcy@univ-rennes1.fr (D. Lorcy).
[1] Fax: + 33 2 23 23 67 38.
[2] Fax: + 33 4 67 14 38 52.

0022-328X/$ - see front matter © 2006 Elsevier B.V. All rights reserved.
doi:10.1016/j.jorganchem.2006.09.034

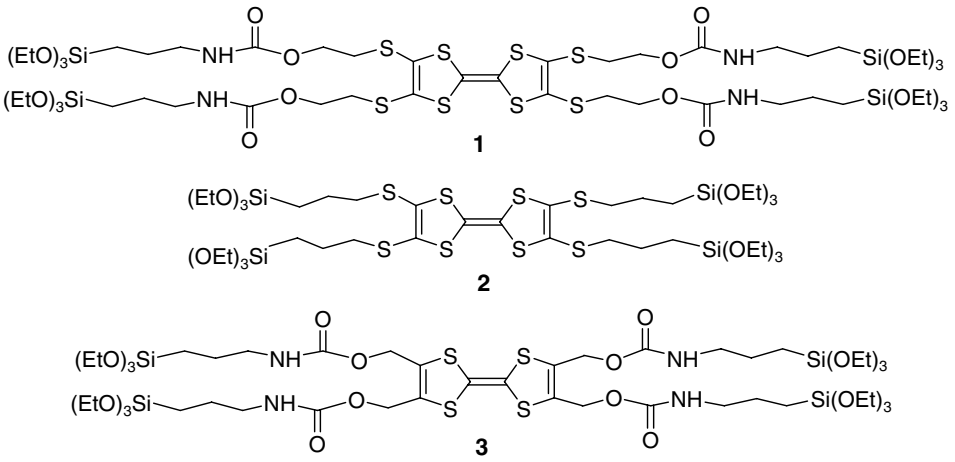

Scheme 1.

polycondensed and presented an organization at both the nanometric (X-ray diffraction) and micrometric scales (birefringence). Among the various organic inorganic nanostructured materials obtained, the tetrakis-substitued derivative **1** exhibited an unprecedented behaviour when observed in polarized light.

In order to determine the driving force of the organization of the organic units within these materials, it appeared very attractive to extend these studies to other TTF precursors, by changing the nature of the spacer between the TTF and the trialkoxysilyl groups. Two parameters can be modified, the ability of the spacer group to give hydrogen bonding phenomenon and the influence of external sulphur atoms. Indeed, S···S interactions involving external sulphur atoms of the fulvalene framework play a role in supramolecular assemblies of TTF derivatives [25]. In this paper, we present the synthesis and electron donating properties of two new tetrakis-substituted trialkoxysilyl TTF (**2**, **3**). On the one hand, we connected the reactive trialkoxysilyl functions to the TTF core through propylthio spacer groups, TTF **2**. On the other hand, a carbamate function was introduced within the side chain between the trialkoxysilyl group and the TTF moiety. We also report their sol–gel hydrolytic polycondensation. The auto-organization of the resulting organic–inorganic hybrid materials is evidenced by X-ray and birefringence experiments.

2. Results and discussion

2.1. Synthetic route to TTF

The alkoxysilyl substituents are known to be highly reactive towards hydrolytic conditions in the presence of various catalysts such as acid, nucleophile or base. Thanks to this reactivity, it is possible to form polysilsesquioxanes in the mild conditions of sol–gel process. The drawback is that the alkoxysilyl substituents have to be grafted on the TTF in the last stage of the synthesis. Therefore in order to reach our goal, we synthesized two precursors, the tetra cyanoethyl-protected TTF thiolate **4** [26] and the tetrahydroxymethyl TTF **5** [27,28] (Scheme 2) according to the literature procedure. Generation of thiolate functions from **4** can be achieved at room temperature with the addition of four equivalents of base which then react with various electrophiles [29]. For our purpose, we used four equivalents of 3-iodopropyl-triethoxysilane as alkylating agent. This electrophile was prepared by nucleophilic substitution of 3-chloropropyl-triethoxysilane with NaI in acetone. Various bases (*t*BuOK, $CsOH \cdot H_2O$, and Cs_2CO_3) and solvent (DMF, THF) have been tested for generating the thiolate. It appeared that DMF was the best solvent and caesium carbonate was the best reactant for the deprotection reaction even if the reaction proceeded more slowly. One can notice that when the catalyst more commonly

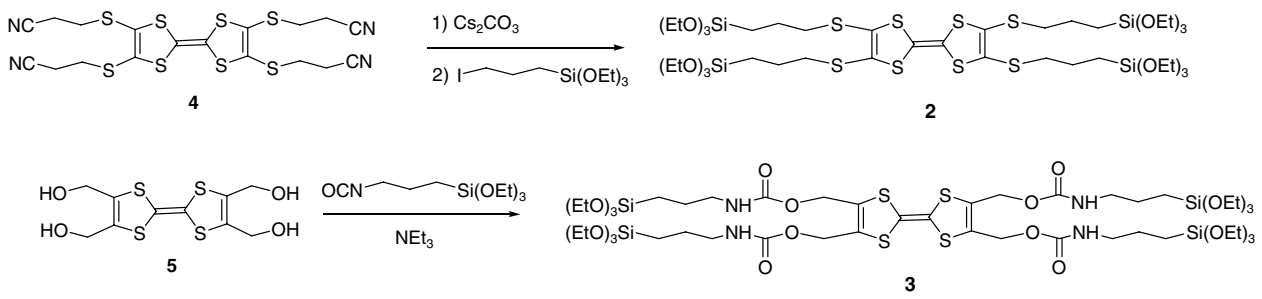

Scheme 2. Synthetic route to precursors **2** and **3**.

employed (CsOH, H_2O) was used, the presence of water in the reagent induces the hydrolytic polycondensation of trialkoxysilane groups and the ratio of polymers was very important.

Concerning the synthesis of TTF **3**, we realized a coupling reaction between the tetrahydroxymethyl-TTF **5** and 3-(triethoxysilyl)propyl isocyanate (Scheme 2). The presence of triethylamine in the medium increased the yield and the kinetics of the reaction [30]. The desired TTF **2**–**3** were purified by chromatography on silica gel and kept in a dry and cold atmosphere to limit uncontrolled and spontaneous polymerisation reactions of the alkoxysilane groups.

2.2. Electrochemical behaviour

The redox properties of these new TTF derivatives together with their precursors were investigated by cyclic voltammetry and the results are summarized in Table 1. Two reversible monoelectronic oxidation waves were observed for TTFs **1**, **2**, **4** and **5** while, by contrast, TTF **3** exhibits three reversible oxidation waves (Fig. 1). Actually, this multi redox processes was quite surprising as usually TTF can be reversibly oxidized to the radical cation and dication. Thus several attempts were realized with various batches of TTF **3** all exhibiting analytical grade and similar results were obtained. This redox behaviour suggests intermolecular interactions between TTF units. Indeed, through space interactions can be observed within dimeric TTF by the splitting of the oxidation steps [31]. Usually, close proximity of the redox cores is at the origin of these interactions either due to a short covalent bridge linking the two TTF cores or through the accommodation of TTFs in a self assembled cage [32]. In our case, this TTF **3** contains four carbamate functions in the flexible side chain and presumably neighbouring carbamate groups tend to form intermolecular H-bonds bringing closer the redox units inducing these interactions. A concentration dependence investigation show that the second wave decreases in intensity upon lowering the concentration of the solution indicating its relationship with oligomeric hydrogen bonded species.

Table 1
Cyclic voltammetry data of TTF, E in V vs. SCE, Pt working electrode with 0.1 M n-Bu_4NPF_6in CH_2Cl_2, scanning rate 100 mV/s

	$E^1(E_{pa}-E_{pc})$	$E^2(E_{pa}-E_{pc})$
1	0.57 (70)	0.88 (80)
2	0.47 (60)	0.78 (80)
3	0.42 (80)/0.60 (70)	0.88 (70)
4	0.67 (80)	0.94 (70)
5	0.23 (60)	0.73 (60)

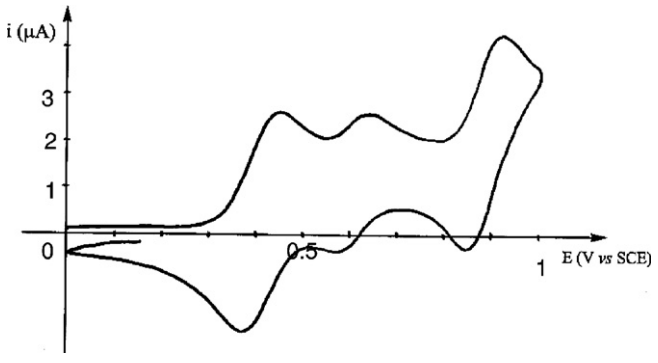

Fig. 1. Cyclic voltammetry of a 7×10^{-4} mol L^{-1} TTF **3** solution in CH_2Cl_2 scanning rate 100 mV/s.

2.3. Sol–gel processing of TTF 1–3

Gel formation from **1**–**3** has been examined under two reaction conditions. The hydrolysis–polycondensation reactions were performed in THF solutions (concentration 0.35 M), using 2% molar of either a nucleophilic catalyst (tetrabutylammonium fluoride, TBAF) or acidic one (HCl) and the stoichiometric amount of H_2O, (1.5 equiv. by $Si(OEt)_3$ group) at room temperature. In most cases, gelation occurred more rapidly using the nucleophilic catalyst than in the presence of the acid catalyst (Table 2). The short gelation times observed for **1** and **3** could originate from the presence of the intermolecular H-bonds between the carbamate units that bring closer the hydrolysable alkoxy groups, thus favouring fast or even spontaneous polycondensation. It is worth noting that in the case of **2** where no carbamate function have been included within the spacer the gelation process can reach 1 h 30 min using HCl. The gels were aged for six days, and then treated as usual to give the xerogels which were used for BET, NMR and X-ray diffraction analyses. Non-porous solids were obtained in all cases ($S_{BET} < 10\ m^2\ g^{-1}$).

The ^{29}Si CP MAS NMR spectra of the xerogels **1X**–**3X** exhibited, in all the cases, two main peaks assigned respectively to T^2 and T^3 substructures (at $\delta \sim -57$ and ~ -66 ppm for **1X**, $\delta \sim -57.5$ and ~ -67.5 ppm for **2X**, and $\delta \sim -56$ and ~ -66 ppm for **3X**). There were no T^0 and T^1 units. The level of condensation, estimated in first approximation by deconvolution [33–35] of spectra are reported in Table 2. Interestingly, all the xerogels prepared in the presence of nucleophilic catalyst (**XA)** were highly polycondensed (range 93–96%), while the xerogels **XB,** obtained under acid catalysis were moderately polycondensed (range 71–76%). A similar observation has been reported in the case of organic–inorganic hybrid materials obtained from bis-substituted(trialkoxysilyl)TTF precursors [24]. Such unusually high level of condensation can be attributed to a pre-organization induced by the interactions between both the TTF cores and the carbamate units. In the case of acid catalysis, the level of condensation is lower since protonation of the donor core by HCl could occur, and therefore a diminution of the catalyst necessary for the overall process [36].

The X-ray powder diffraction diagrams of these materials are given in Fig. 2. Like for all the other nanostructured hybrid materials [6,15], they did not exhibit narrow Bragg

Table 2
Characteristics of gels and xerogels

Precursor	Xerogel	Catalyst	Gel time (min)	Birefringence Δn ($\times 10^3$)	^{29}Si CP MAS NMR (%)				L.C.[a] (%)
					T^0	T^1	T^2	T^3	
1	**1XA**	TBAF	2	5	0	0	13	87	96
1	**1XB**	HCl	2	5.1	0	0	72	28	76
2	**2XA**	TBAF	10	3.2	0	0	21	79	93
2	**2XB**	HCl	90	3.5	0	0	88	12	71
3	**3XA**	TBAF	2	3.6	0	0	13	87	96
3	**3XB**	HCl	8	3.9	0	0	75	25	75

[a] Level of condensation.

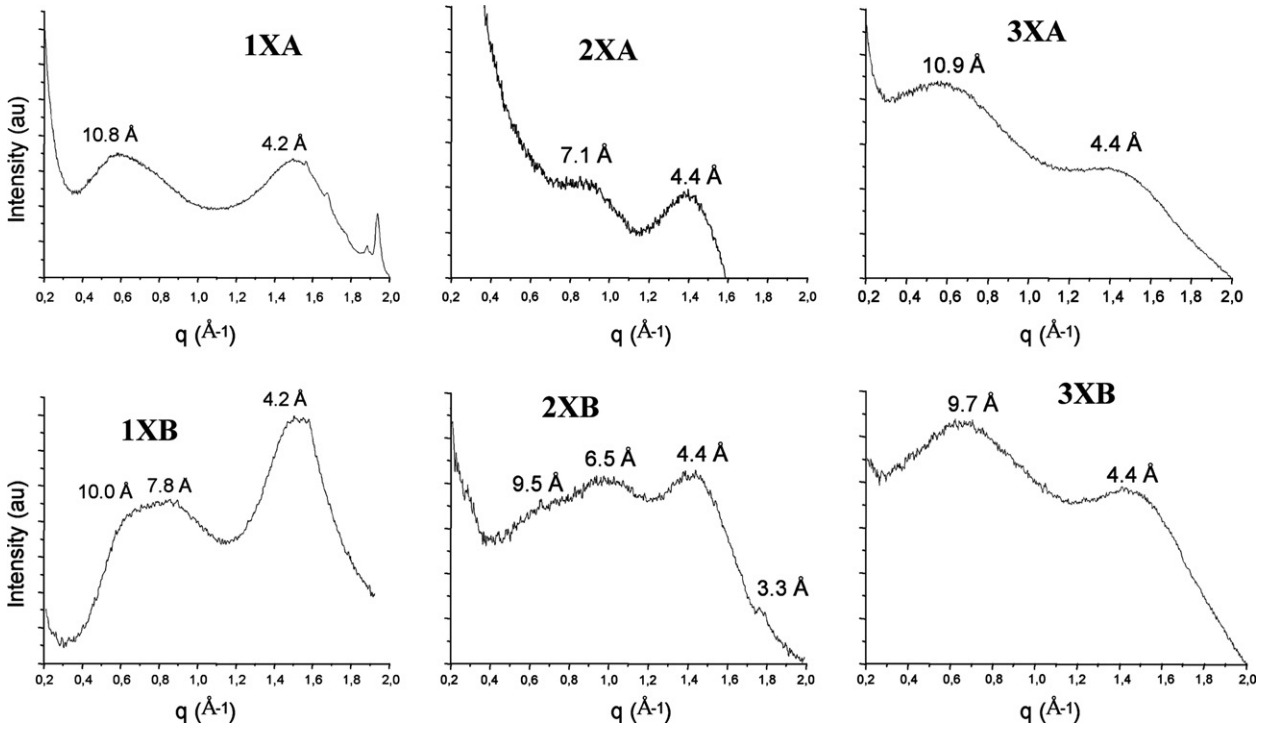

Fig. 2. X-ray diffraction diagrams for xerogels **1X**–**3X**.

reflexions. For each sample, the presence of broad reflexions only rules out the occurrence of long-range order in the condensed state. However, as a first approximation assuming Bragg's law a priori, the distances associated with the q values were determined ($d = 2\pi/q$). Apart for **1XA** previously reported [23], no sharp signals or broad ones were observed on all the powder X-ray diffraction diagrams of the xerogels when analysed from 0.04 to 0.2 $Å^{-1}$. As can be seen in Fig. 2, when analyzed between 0.2 and 2 $Å^{-1}$ the nature of the catalyst used for the hydrolysis–polycondensation reaction appeared to have a significant influence on the organization at the nanometric scale in the case of **2X** since the X-ray diffraction patterns of the corresponding solids (**XA** and **XB**) are different. Concerning **1XA** and **1XB** the difference observed was in the relative intensities of the two main peaks while for **3XA** and **3XB** no significant differences were observed since the shapes of the diagrams were similar and signals were located at close q values. Interestingly, only the xerogels where intermolecular H bonds are impossible (**2X**) exhibit very different diagrams with the nature of the catalyst. S···S interactions being weaker than the hydrogen bonds it can be postulated that these weak interactions between the precursors **2**, prior to gelation process, can be easily modulated with the conditions used for hydrolysis–polycondensation . In all cases a broad signal centered at 1.5 $Å^{-1}$, (4.2 Å) for solids **1X**, and at 1.43 $Å^{-1}$, (4.4 Å) for xerogels **2X** and **3X**, was present as already observed in all other nanostructured silica-based hybrid materials, and was attributed to the contribution of Si–O–Si units [37]. However in the case of **1XB**, considering the relative intensity between the two broad signals located at 4.2 Å, it was possible to conclude that in this case, this signal could correspond to the overlap of the Si–O–Si units contribution and of another signal corresponding to a distance characteristic of the organic units. A comparison between the xerogels **1XA** and **1XB** is of

great interest since the level of organization appears to highly depend on the nature of the catalyst employed for polycondensation. As already reported [23] the nucleophilic catalyst leads to a high level of organization at the nanometric scale, a stacking of 28 TTF units has been evidenced. In contrast, with acid catalyst, such organization was not observed, the diagram exhibiting only a broad signal presenting two shoulders at $\sim$0.63 $Å^{-1}$ (10.0 Å) and $\sim$0.80 $Å^{-1}$ (7.8 Å). This could arise from the protonation of the TTF core by HCl that induced a distortion of the core and thus prevented the stacking of TTF units [36].

When compared with **1**, the precursor **2** presented the same TTF core and two shorter arms without possibility of H-bonding. In this case, the X-Ray diffraction diagrams of **2XA** and **2XB** were also very different. For **2XA**, only one broad signal at $\sim$0.88 $Å^{-1}$ (7.1 Å) was observed in addition to the one at 1.43 $Å^{-1}$ (4.4 Å), whereas **2XB** exhibited three broad signals at $\sim$0.66 $Å^{-1}$ (9.5 Å), 0.97 $Å^{-1}$ (6.5 Å) and 1.90 $Å^{-1}$ (3.3 Å). The last signal at 3.3 Å should correspond to the distance between two planes of TTF as already reported in the literature [38,39]. At present it is difficult to attribute the two other signals, however they could correspond to the distance between planes containing sulfur atoms taking into account the distances determined by computer calculations.

In the case of **3X**, no main differences were observed (Fig. 2), such result could arise from a pre-organization existing in the precursor and favored by the presence of shorter arms and H-bonding between carbamate units, and which is in good agreement with its electrochemical behavior.

The observation by microscopy in polarized light gave information about the micrometric scale order in the solids. A small part of the gelation mixture was introduced separately into thin Teflon-coated cells. Teflon was chosen because of its chemical stability [40]. The initial solutions were completely dark when analyzed by polarized optical microscopy; this observation is characteristic of an isotropic medium. Transparent gels formed as evidenced by the absence of hydrodynamic movement, allowing a clear observation and measurements of the birefringence. Birefringence was observed for all the gels (**1X**–**3X**) and one can notice that the values of birefringence (Δn) for the gels prepared with the acid catalyst are slightly higher than the one prepared with the nucleophilic catalyst (Table 2). These values of birefringence (Δn) indicate the formation of anisotropic organized materials. Another interesting point is to compare the values of birefringence with the nature of the spacer between the TTF and the trialkoxysilyl groups. Indeed, the lowest birefringence was observed for the gels **2X** ($3.2–3.5 \times 10^{-3}$) with only a propylthio spacer.

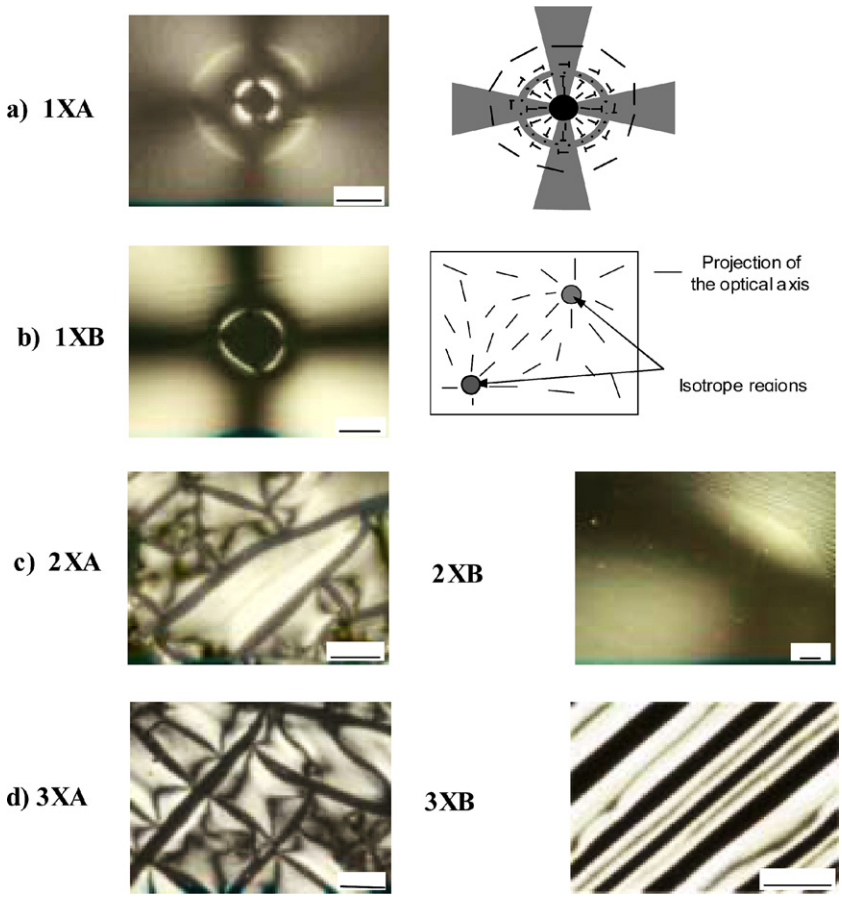

Fig. 3. Birefringence pictures for xerogels **1X**–**3X**.

The Δn values increased slightly for the gels **3X** (3.6–3.9×10^{-3}) where only a carbamate function was introduced and the highest values were obtained for the gels **1X** where the spacer combines external sulfur and carbamate moieties. This indicates that in **1X** these values are the result of both contributions which are the S···S interactions and the intermolecular H-bonds. It can be underlined also that all these tetrasubstituted precursors, TTF **2** and **3,** give rise to gels exhibiting higher birefringence values than the bis-substituted derivatives with the same spacer group as in **1** [24].

The solids **XA** and **XB** exhibited different birefringence morphologies depending on the nature of the catalyst used for polycondensation reaction (Fig. 3).

In the case of **1XA** an unprecedented behavior was observed [23] and we have reported the different orientations of the optical axis (Fig. 3a). For **1XB**, the situation was different since the optical axis was oriented radially around the circular isotropic regions (Fig. 3b), as usually observed for such birefringence morphologies. When compared to **1XA**, the solid **1XB** appeared less organized because of the distortion of the TTF core due to protonation by HCl [36] . The solid **2XA** exhibited a classical behavior with the presence of cracks and birefringent chunks of gel (Fig. 3c), the optical axis being oriented perpendicular to the cracks. In contrast, for **2XB** a birefringence without cracks was observed. Finally **3XA** and **3XB** presented the classical phenomenon of cracks and birefringent chunks of gel. In the case of acid catalyst the cracks were regular and parallel one to each other (Fig. 3d). The optical axis was oriented perpendicular to the cracks and the organic units were stacked inside the aggregates.

3. Conclusion

Tetrasubstituted (trialkoxysilyl)TTF derivatives have been prepared in order to analyze the influence of various spacers between the TTF skeleton and the silicon atoms on the organization of the organic units in silica-based hybrid materials. Whatever the nature of the spacer, a drastic effect of the catalyst used to promote the hydrolytic polycondensation was observed on (i) the level of condensation and (ii) the mesoscopic organization of the solids. The TBAF nucleophilic catalyst gives rise to a higher polycondensation degree than the HCl acid catalyst. An anisotropic organization, evidenced by observation of birefringence in the gels, increases with the nature and number of specific moieties involved in the supramolecular organization during the gelation process, that is, outer sulphur atoms for stronger van der Waals interactions, carbamate groups for stronger hydrogen bonding and their combination. The results reported here confirm the fact that the different scales of organization observed for nanostructured hybrid materials (nanometric and micrometric) are independent one from each other. They correspond to different phases of the process that are governed by the different parameters which control the kinetics of polycondensation.

4. Experimental

4.1. General methods

THF was distilled from sodium-benzophenone prior to use. Methanol was dried over calcium and distilled. Toluene was dried over sodium wire. DMF was stirred over CaO overnight and distilled prior to use. All reagents were commercialy available and used without purification. tetra-hydroxymethyl-TTF (**5**) [27,28], tetra-cyanoethylthio-TTF (**4**) [26] were synthesized according to the literature procedure. ^{1}H NMR and ^{13}C NMR spectra were recorded on Bruker ARX 200 spectrometer. Chemical shifts are quoted in parts per million (ppm) referenced to tetramethylsilane. The ^{29}Si CP MAS NMR spectra were recorded on a Bruker Avance 300 spectrometer operating at 60 MHz using a recycling delay of 10 s and a contact time of 5 ms. The spinning rate was 5 kHz. Chemical shifts are given relative to tetramethylsilane. Mass spectra were recorded with Varian MAT 311 instrument by the Centre Régional de Mesures Physiques de l'Ouest, Rennes. Elemental analysis were performed at the Laboratoire Central de Microanalyse du CNRS, Lyon. TLC was performed with Merck Kieselgel 60 F_{254} plates, with viewing under ultraviolet light (254 nm). Chromatography was performed using silica gel Merck 60 (70–260 mesh). Cyclic voltammetry was carried out on a 10^{-3} M solution of TTF derivative in CH_2Cl_2 containing 0.1 M n-Bu_4NPF_6 as supporting electrolyte. Voltammograms were recorded at 0.1 V s^{-1} at a platinum disk electrode (1 mm^2). Potentials were measured versus Saturated Calomel Electrode (SCE). The nitrogen adsorption–desorption isotherms at 77.35 K were recorded on a Micromeritics Gemini III 2375 apparatus. The specific surface area was determined using the BET equation. The X-ray experiments were performed on powders of solids in a Lindeman tube with an imaging plate two-dimensional detector (Marresearch 2D "Image-Plate") with a rotating anode apparatus (Rigaku RU 200). The radiation used was Cu Kα ($\lambda = 1.5418$ Å). Optical properties of the materials were observed with a Laborlux12POLS polarizing microscope. Photographs were taken using a Leica wild MPS28 camera. The birefringence Δn of the gels was obtained from the expression $\Delta l = (\Delta n)d$, where Δl is the optical path difference and d is the cell thickness which is evaluated by UV–Vis spectroscopy (~15 μm). Δl was measured by a Berek compensator.

4.2. Synthesis of [2,2′-bi-1,3-dithiole-4,4′,5,5′-tetrayltetrakis(thiopropane-3,1- diyl)]tetrakis (triethoxysilane) (2)

To a solution of tetra-(cyanoethylthio)-TTF (**4**) (1 mmol) in 50 mL of DMF was added under argon

Cs_2CO_3 (4.2 mmol). The mixture was refluxed for 3 h after which 3-iodopropyltriethoxysilane (4.4 mmol) was added. Stirring was continued for 1 h at RT. Solvents were removed by rotary evaporation and the residue was diluted with CH_2Cl_2, filtered and concentrated. Chromatography over silica gel (CH_2Cl_2/Et_2O, 7:1) afforded **2** (0.88 g, 77%) as an orange oil. R_f 0.82. ^1H NMR (200 MHz, $CDCl_3$): $\delta = 0.74$ (m, 8H, $SiCH_2$), 1.21 (t, $J = 7.0$ Hz, 36H, CH_3), 1.76 (tt, $J = J = 7.3$ Hz, 8H, CH_2), 2.83 (t, $J = 7.3$ Hz, 8H, SCH_2), 3.80 (q, $J = 7.0$ Hz, 24H, OCH_2). ^{13}C NMR (50 MHz, DMSO-*d*6): $\delta = 9.8$, 18.9, 24.0, 39.1, 58.6, 110.6, 128.0. ^{29}Si NMR (60 MHz, $CDCl_3$): $\delta = -46.25$ (s). Found: $M^{+\cdot}$, 1148.2854. $C_{42}H_{84}O_{12}Si_4S_8$ requires M, 1148.2806. Found: C, 43.68; H, 7.36; S, 21.84%. $C_{42}H_{84}O_{12}Si_4S_8$ requires C, 43.87; H, 7.36; S, 22.31.

4.3. Synthesis of 2,2′-bi-1,3-dithiole-4,4′,5,5′-tetrayltetrakis(methylene)]tetrakis{[3-(triethoxysilyl)propyl] carbamate} (3)

To a solution of tetra-(hydroxymethyl)-TTF (**5**) (1 mmol) in 10 mL of anhydrous THF was added under argon 3-(triethoxysilyl)propyl isocyanate (4.4 mmol) and triethylamine (4.4 mmol). The mixture was refluxed for 24 h. Evaporation of the solvent followed by chromatography over silica gel (CH_2Cl_2/Et_2O 2:1) afforded **3** (0.73 g, 56%) as an orange thick oil. R_f 0.59. ^1H NMR (200 MHz, $CDCl_3$): $\delta = 0.65$ (m, 8H, $SiCH_2$), 1.23 (t, $J = 7.0$ Hz, 36H, CH_3), 1.65 (tt, $J = J = 7.1$ Hz, 8 H, CH_2), 3.19 (dt, $J = J = 7.1$ Hz, 8H, NCH_2), 3.84 (q, $J = 7.0$ Hz, 24H, CH_2), 4.88 (s, 8H, OCH_2), 5.18 (t, $J = 7.1$ Hz, 4H, NH). ^{13}C NMR (50 MHz, $CDCl_3$): $\delta = 8.0$, 18.7, 23.6, 43.9, 58.9, 65.0, 108.7, 130.4, 155.9. ^{29}Si NMR (60 MHz, $CDCl_3$): $\delta = -45.90$ (s). Found: $M^{+\cdot}$, 1312.4632. $C_{50}H_{96}N_4O_{20}S_4Si_4$ requires M, 1312.4578. Found: C, 45.95; H, 7.44; N, 4.27; S, 9.51%. $C_{50}H_{96}N_4O_{20}S_4Si_4$ requires C, 45.71; H, 7.36; N, 4.26; S, 9.76.

4.4. General procedure for the synthesis of gels and xerogels

The preparation of the xerogels was carried out according to the following general procedure. The preparation of **1XA** is given as an example: compound **1** (0.208 g, 0.139 mmol) and dried THF (198 μL) were introduced into a Schlenk tube. 198 μL of a solution containing 3 μL (3μmoles) of TBAF (1 M in THF), H_2O (15 μL, 0.834 mmol) and dried THF (180 μL) were added. After homogenization, a part of this mixture was introduced by capillarity into the cell, and the remaining solution was kept in the Schlenk tube. After the sol-gel transition, (2 min), the gel was aged 6 days. Then, the gel obtained in the Schlenk tube was crushed and washed twice with acetone, ethanol and diethyl ether, and the resulting powder was dried at 120°C in vacuo for 3 h yielding a xerogel.

1XA: orange powder. 0.140 g (0.137 mmol); Yield: 99%. ^{29}Si CP MAS NMR (δ ppm, 60 MHz): −56.9 (T^2), −66.4 (T^3). $S_{BET} < 10\ m^2\ g^{-1}$.

1XB: 0.208 g (0.139 mmol) of **1** in 198 μL of THF and 198 μL of a solution containing 3 μL of HCl, 15 μL of H_2O and 180 μL of THF gave a dark orange gel after 5 min. **1XB**: dark orange powder. 0.142 g (0.58 mmol); Yield: 100%. ^{29}Si CP MAS NMR (δ ppm, 60 MHz): −57.3 (T^2); 65.7 (T^3). $S_{BET} < 10\ m^2\ g^{-1}$.

2XA: 0.300 g (0.261 mmol) of **2** in 373 μL of THF and 340 μL of a solution containing 5 μL of TBAF, 28 μL of H_2O and 340 μL of THF gave an orange gel after 10 min. **2XA**: orange powder. 0.180 g (0.255 mmol); Yield: 98%. ^{29}Si CP MAS NMR (δ ppm, 60 MHz): −57.5 (T^2); 67.3 (T^3). $S_{BET} < 10\ m^2\ g^{-1}$.

2XB: 0.300 g (0.261 mmol) of **2** in 373 μL of THF and 340 μL of a solution containing 5 μL of HCl, 28 μL of H_2O and 340 μL of THF gave a dark orange gel after 90 min. **2XB**: dark orange powder. 0.175 g (0.248 mmol); Yield: 95%. ^{29}Si CP MAS NMR (δ ppm, 60 MHz): −58.1 (T^2); 67.8 (T^3). $S_{BET} < 10\ m^2\ g^{-1}$.

3XA: 0.417 g (0.318 mmol) of **3** in 454 μL of THF and 413 μL of a solution containing 6 μL of TBAF, 35 μL of H_2O and 413 μL of THF gave an orange gel after 2 min. **3XA**: orange powder. 0.260 g (0.300 mmol); Yield: 95%. ^{29}Si CP MAS NMR (δ ppm, 60 MHz): −57.3 (T^2); 65.7 (T^3). $S_{BET} < 10\ m^2\ g^{-1}$.

3XB: 0.417 g (0.318 mmol) of **3** in 454 μL of THF and 413 μL of a solution containing 6 μL of HCl, 35 μL of H_2O and 413 μL of THF gave a dark orange gel after 8 min. **3XB**: dark orange powder. 0.254 g (0.292 mmol); Yield: 92%. ^{29}Si CP MAS NMR (δ ppm, 60 MHz): −56.5 (T^2); 65.8 (T^3). $S_{BET} < 10\ m^2\ g^{-1}$.

References

[1] C.J. Brinker, G.W. Scherer, Sol–Gel Science: The Physics and Chemistry of Sol–Gel Processing, Academic Press, 1990.
[2] D.A. Loy, K.J. Shea, Chem. Rev. 95 (1995) 1431.
[3] C. Sanchez, F. Ribot, New J. Chem. 18 (1994) 1007, special issue.
[4] K.J. Shea, D.A. Loy, Mater. Res. Bull. 5 (2001) 358.
[5] B. Boury, R.J.P. Corriu, Chem. Commun. (2002) 795, and references cited.
[6] B. Boury, R.J.P. Corriu, in: Z. Rappoport, Y. Apeloig (Eds.), Supplement Si: the Chemistry of Organosilicon Compounds, Wiley, Chichester, 2001 (Chapter 10, p. 565 and references cited).
[7] C. Sanchez, P. Gomez-Romero (Eds.), Functional Hybrid Materials, Wiley VCH, Weinheim, 2004, p. 50.
[8] C. Sanchez, B. Julian, P. Belleville, M. Popall, J. Mater. Chem. 15 (2005) 3559.
[9] B. Boury, F. Ben, R.J.P. Corriu, P. Delord, M. Nobili, Chem. Mater. 14 (2002) 730.
[10] B. Boury, R.J.P. Corriu, Chem. Rec. 3 (2003) 120, and references cited.
[11] B. Boury, F. Ben, R.J.P. Corriu, Adv. Mater. 14 (2002) 101.
[12] G. Cerveau, R.J.P. Corriu, E. Framery, F. Lerouge, Chem. Mater. 16 (2004) 3794.
[13] G. Cerveau, R.J.P. Corriu, E. Framery, F. Lerouge, J. Mater. Chem. 14 (2004) 3019.
[14] F. Lerouge, G. Cerveau, R.J.P. Corriu, J. Mater. Chem. 16 (2006) 90.

[15] F. Lerouge, G. Cerveau, R.J.P. Corriu, New J. Chem. 30 (2006) 272, and references cited.
[16] J.J.E. Moreau, L. Vellutini, M.W.C. Man, C. Bied, J.-L. Bantignies, P. Dieudonne, J.-L. Sauvajol, J. Am. Chem. Soc. 123 (2001) 7957.
[17] J.J.E. Moreau, L. Vellutini, M.W.C. Man, C. Bied, J. Am. Chem. Soc. 123 (2001) 1509.
[18] J.J.E. Moreau, L. Vellutini, M.W.C. Man, C. Bied, Chem. Eur. J. 9 (2003) 1594.
[19] C. Bied, J.J.E. Moreau, L. Vellutini, M.W.C. Man, J. Sol-Gel Science and Technology 26 (2003) 583.
[20] J.J.E. Moreau, B.P. Pichon, M. Wong Chi Man, C. Bied, H. Pritzkow, J.-L. Bantignies, P. Dieudonne, J.-L. Sauvajol, Angew. Chem., Int. Ed. 43 (2004) 203.
[21] J.J.E. Moreau, B.P. Pichon, C. Bied, M. Wong Chi Man, J. Mater. Chem. 15 (2005) 3929.
[22] J.J.E. Moreau, L. Vellutini, P. Dieudonne, M. Wong Chi Man, J.-L. Bantignies, J.-L. Sauvajol, C. Bied, J. Mater. Chem. 15 (2005) 4943.
[23] G. Cerveau, R.J.P. Corriu, F. Lerouge, N. Bellec, D. Lorcy, M. Nobili, Chem. Commun. (2004) 396.
[24] N. Bellec, F. Lerouge, B. Pichon, G. Cerveau, R.J.P. Corriu, D. Lorcy, Eur. J. Org. Chem. (2005) 136.
[25] C. Rovira, Chem. Rev. 104 (2004) 5289.
[26] N. Svenstrup, K.M. Rasmussen, T.K. Hansen, J. Becher, Synthesis 8 (1994) 809.
[27] M.A. Fox, H.-I. Pan, J. Org. Chem. 59 (1994) 6519.
[28] M. Salle, A. Gorgues, M. Jubault, K. Boubeker, P. Batail, Tetrahedron 48 (1992) 3081.
[29] K.B. Simonsen, J. Becher, Synlett (1997) 1211, and references cited.
[30] P. Hesemann, J.J.E. Moreau, Tetrahedron Asym. 11 (2000) 2183.
[31] M. Iyoda, M. Hasegawa, Y. Miyake, Chem. Rev. 104 (2004) 5085.
[32] M. Yoshizawa, K. Kumazawa, M. Fujita, J. Am. Chem. Soc. 127 (2005) 13456.
[33] CP MAS is generally not quantitative; however, when compared with single-pulse experiments that allow a quantitative determination, no significant variation in relative peak intensity was observed in the case of such alkylene or arylene hybrid solids [34,35]. Moreover, since materials of similar precursors are compared, it can be assumed that relative peak intensity can be used to show a variation of the level of condensation between them.
[34] G. Cerveau, R.J.P. Corriu, C. Lepeytre, P.H. Mutin, J. Mater. Chem. 8 (1998) 2707.
[35] H.W. Oviatt, K.J. Shea, J.H. Small, Chem. Mater. 5 (1993) 943.
[36] M. Giffard, P. Alonso, J. Garin, A. Gorgues, T.P. Nguyen, P. Richomme, A. Robert, J. Roncali, S. Uriel, Adv. Mater. 6 (1994) 298.
[37] B. Boury, R.J.P. Corriu, P. Delord, V. Le Strat, J. Non-Cryst. Solids 265 (2000) 41.
[38] H. Kobayashi, A. Kobayashi, Y. Sasaki, G. Saito, H. Inokuchi, Bull. Chem. Soc. Jpn. 59 (1986) 301.
[39] S. Matsumiya, A. Izuoka, T. Sugawara, T. Taruishi, Y. Kawada, Bull. Chem. Soc. Jpn. 66 (1993) 513.
[40] B. Boury, R.J.P. Corriu, P. Delord, M. Nobili, V. Le Strat, Angew. Chem., Int. Ed. 38 (1999) 3172.